LVRT Capability Assessment of FSIG-based Wind Turbine Utilizing UPQC and SFCL

Amir Hasan Moghadasi, *Student Member, IEEE,* Arif Islam, *Member, IEEE,* and Mohamadhadi Amini, *Student Member, IEEE.*

***Abstract*—This paper investigates a fixed-speed induction generator (FSIG)-based wind turbines in effective combination with unified power quality conditioner (UPQC) and resistive superconducting fault current limiter (RSFCL). The UPQC control scheme is introduced to ensure the maximum low voltage ride-through (LVRT) enhancement of the FSIG-based wind turbine by compensating the voltage sag at the point of common coupling (PCC). Additionally, a realistic estimation of the volt-ampere rating requirements of UPQC for this type of application is carried out. In this paper the utilization of RSFCL is proposed to limit excessive current in the event of the fault. For this purpose, the electro-thermal model of the SFCL is implemented in PSCAD/EMTDC software as a component to verify SFCL damping performance. The obtained results confirm that the SFCL can not only reduce the volt-ampere rating of the UPQC, thereby reducing the installation cost but also aid to the LVRT capability improvement of the wind turbine as well as dynamic performance of the induction generator.**

***Index Terms*—Low Voltage Ride-Through (LVRT), Power quality, Resistive Superconducting Fault Current Limiter (RSFCL), Unified Power Quality Conditioner (UPQC).**

I. Introduction

WIND turbine with the grid-connected mode of operation plays a significant role toward in sustainable energy development in the future power system. Network faults and the corresponding voltage dips may cause many issues for the power system, such as disconnecting a large wind farm and consequently serious effects on the power system operation. Therefore, there is a crucial requirement to develop upgraded grid codes, especially topics concerning the grid voltage support under various fault conditions, which is called low voltage ride-through (LVRT) capability. A practical paradigm of the LVRT curve defined by the US grid code has been discussed in [1]. If the voltage of wind farm remains at the level greater than 15% of nominal voltage for a period less than 0.625 s, the plant should be connected to the grid.

The most conventional wind farms are based on fixed-speed induction generator (FSIG)-type directly connected to the grid which is considered as simplest and most cost-effective technology among various wind generators [2]. Due to this generator type draws reactive power during the fault period and even after fault clearance; not only it cannot meet the grid code requirements, but also it exacerbates the voltage sag condition by absorbing reactive power. In order to improve LVRT capability of FSIG-based wind turbine, several methods have been already deployed, such as fast pitching of the turbine blades [3], using commercially available FACTS devices [4-6], and implementing energy storage systems [7]. The unified power quality conditioner (UPQC) has been widely studied as an ultimate device to improve power quality challenges, such as voltage sag and harmonic current [8-10]. However, the capital cost involved in the installation of this device is higher than any other FACTS devices because of using two converters. A resistive superconducting fault current limiter (RSFCL) is an appliance installed in electric power system for limiting the excessive current by switching into a high-impedance state during a fault event. It has been documented that the SFCL has many advantageous features such as current detecting and recovering automatically, and faster excessive current damping performances [10], [11].

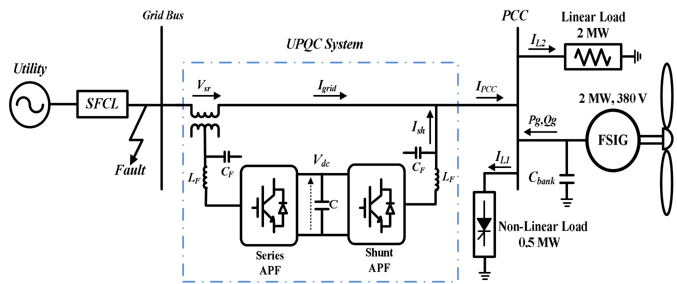

Fig. 1. Structure of the proposed system: FSIG-based wind turbine with UPQC and SFCL connected to the grid.

The general framework of this study is illustrated in Fig. 1. In this paper, the cost effective solution for FSIG-based wind turbine is proposed to fulfill grid code requirements. This work accomplished by installation of UPQC at the wind farm terminal in order to ameliorate both power quality and LVRT capability of wind farm. The additional cost to integrate the UPQC can be decreased by utilizing the RSFCL as self-healing equipment which is the main motivation of this effort. To ensure the validity of the proposed technique, the whole system is modelled using PSCAD/EMTDC software

II. Wind Turbine Model

A significant number of the wind farms in operation are equipped with fixed-speed squirrel-cage induction generators and the capacitor banks providing the generator reactive power requirements. The nonlinear model of the wind turbine commonly simplified to a static model of the aerodynamic

The authors are with the Electrical Engineering Department, Center of Energy, Power & Sustainability (EPS), Florida International University (FIU), Miami 33174, USA (e-mail: amogh004@fiu.edu, arislam@fiu.edu mamin006@fiu.edu).

978-1-4799-6415-4/14/$31.00 ©2014 IEEE

rotor, a two-mass model of the drive train and a third-order model of induction generator.

A. Aerodynamic Model

The mechanical power extracted by a wind turbine from the wind is expressed by the well-known formula:

$$P_w = \frac{1}{2}\rho A V_w^3 C_p \tag{1}$$

where ρ is the air density, A is the area of the rotor disk, V_w is the wind speed and C_p is the power coefficient. The power coefficient characterizes the rotor aerodynamics as a function of both tip speed ratio and the blade pitch angle. The tip speed ratio is defined as the relationship between rotor blade speed and the wind speed [12].

B. Drive Train System

The drive train of the wind turbine generator is designated by a two-mass model [13] which can be represented by (2)-(4).

$$2H_r \frac{d\omega_r}{dt} = T_{wt} - T_m \tag{2}$$

$$2H_e \frac{d\omega_e}{dt} = T_m - T_e \tag{3}$$

$$T_m = D_m(\omega_r - \omega_e) + K_m \int (\omega_r - \omega_e)\ dt \tag{4}$$

where T_{wt}, T_m and T_e are the mechanical torque from the wind turbine rotor shaft, the mechanical torque from the generator shaft and generator electrical torque, respectively. Moreover H_r is wind turbine inertia, H_e is generator inertia and, K_m and D_m are the stiffness and damping of mechanical coupling.

C. Generation System Model

In power system stability studies, the third-order model of FSIG can be achieved by neglecting the stator flux transients in the voltage relations and eliminating the rotor currents. However, the equations used for squirrel cage induction generator modeling are described in [14]. Also, Fig. 2 shows the control scheme of pitch angle regulator of the wind turbine. The inputs to the model are the mechanical speed of the machine ωm and the power output of the machine Pg.

III. The Proposed UPQC System

In this study, the UPQC topology is composed of the integration of a series-active and a shunt-active power filters (APFs) connected back to back to a common DC-link which is recognized as the most complicated power quality improvement, and probably the most expensive one. The major goal of the series APF is to isolate between a sub-transmission system and a distribution system from a harmonic point of view. It is additionally able of compensating voltage imbalance, voltage adjustment and harmonic at the utility-customer at the PCC. Whereas, the shunt-APF draws current harmonics, compensates for reactive power and negative-sequence current inserted by the load. It also controls and manages the DC-link voltage of capacitor to the desired value.

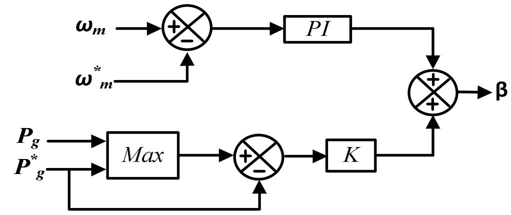

Figure 2. Pitch angle Control used in FSIG-based wind turbine.

The passive filters are also utilized for cancellation of the high switching frequency generated from the shunt and series APF_S. Fig. 1 shows the configuration of the proposed system with UPQC is located between the grid bus and wind turbine terminal.

A. Control Scheme of the Proposed System

The series APF operates as a controlled voltage source, keeping the load voltage sinusoidal and at the given constant voltage level. Furthermore, it inserts a voltage equal to the difference of the grid voltage and the nominal load voltage. In order to suppress the harmonic current and compensate the reactive power concurrently, the shunt active power filter is proposed. The operation of the shunt APF is the same as a current source parallel with the non-linear load. In this study, a modified methodology with instantaneous power theory (*p–q* theory) is introduced, as an efficacious approach to the non-linear three-phase systems assessment as well as the shunt APF control [3].

$$\begin{bmatrix} p \\ q \end{bmatrix} = \begin{bmatrix} v_\alpha & v_\beta \\ -v_\beta & v_\alpha \end{bmatrix} \begin{bmatrix} i_\alpha \\ i_\beta \end{bmatrix} \tag{9}$$

$$\begin{bmatrix} i^*_\alpha \\ i^*_\beta \end{bmatrix} = \frac{1}{{v_\alpha}^2 + {v_\beta}^2} \begin{bmatrix} v_\alpha & -v_\beta \\ v_\beta & v_\alpha \end{bmatrix} \begin{bmatrix} \tilde{p} - \overline{p}_{loss} \\ q \end{bmatrix} \tag{10}$$

The overall control scheme including series APF and shunt APF controller is shown Fig. 3, where, $V^*_{PCC}=V_m \sin(\omega t+k\pi/3)$, $k=0,1,2$, is the reference PCC voltage and V_F is the generated voltage with series APF. Also, $V_{dc\text{-}ref}$ is the reference value capacitor voltage and P_{loss} is converters' switching losses.

IV. Electro-Thermal Modeling of a Resistive SFCL

Practically, HTS fault current limiters (FCLs) have been classified into the resistive, inductive, and hybrid types [15-17]. In the three mentioned types of SFCL, the resistive type can protect the system against the fault current instantaneously by a considerable increment in the resistance. This type of SFCL is not structurally intricate. Resistive type SFCL also can be switched to the normal operation condition autonomously after barricading the fault current. Hence, the damping performance of RSFCL is recognized as multisided cooperation between the fault current magnitude values, thermal properties, and the variable resistance of HTS substrate.

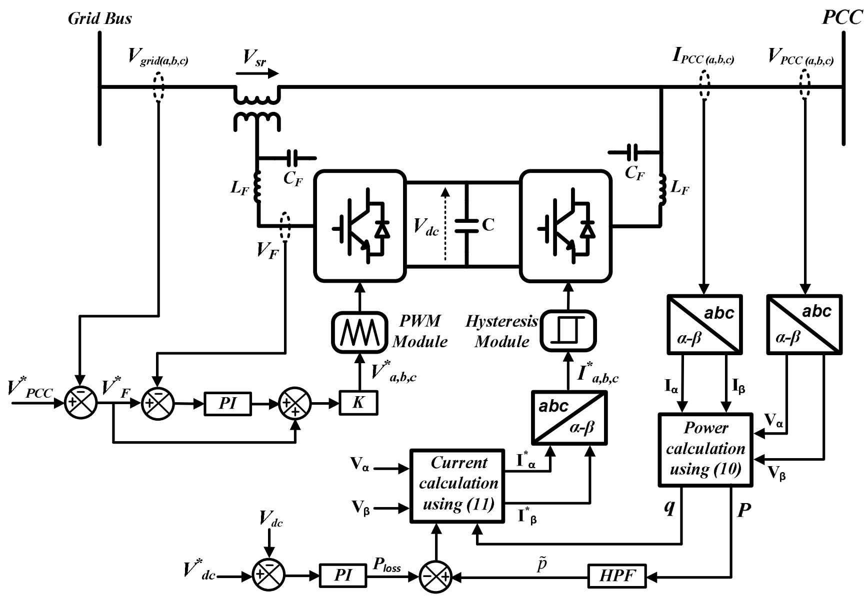

Fig. 3. Proposed control structure of the UPQC to compensate voltage sag and current harmonic.

The RSFCL is based on superconducting bars or double non-inductive spirals [16] for effective elimination of inductance. YBCO coated conductors are generally used for resistive type of SFCLs. The current limiting behavior of the RSFCL can be practically subdivided into superconducting state, flux flow state and normal conducting state in which is assumed 1) superconducting state at a temperature and a current under the critical rate; 2) flux flow state at a current over the critical value but temperature under the critical rate; and 3) normal conductive state at a temperature higher the critical amount. Detailed formulation can be found in [11].

V. Numerical Simulation Analysis

In this section, in order to verify the effectiveness of the proposed structure shown in Fig. 1, simulation studies were carried out using PSCAD/EMTDC. In the simulation, utilizing the proposed structure, the LVRT capability and dynamic stability of the SFIG-based wind is enhanced. A fixed-speed squirrel-cage induction generator (2MW) is directly connected to the PCC. For the reactive power compensation purpose, a capacitor bank (C_{bank}) is connected to the terminal of induction generator. The value of the capacitor is chosen so that the power factor of the wind generator during the rated operation becomes unity.

The total output power of a wind turbine is supplied to the resistive load (L_2, 2MW) installed at the PCC. Moreover, the nonlinear and sensitive load of a three-phase diode bridge (L_1, 50 kVA) supplied by the grid was considered to affirm the ability of UPQC in reducing current harmonics. Finally, the grid is represented as an infinite source with the fixed frequency of 50 Hz and voltage of 380 V interconnected to the infinite bus via the RSFCL.

Table I and table II show wind turbine characteristics and RSFCL parameters, respectively. The detailed information about UPQC parameters can be found in [10] in which supply voltage is 380 V, the resistance and inductances of the system are 0.006 Ω and 0.02 *mH,* respectively.

TABLE I
CHARACTERISTICS OF THE WIND FARM INDUCTION GENERATOR

Symbol	Quantity	Value
P_{rated}	Rated generator power	2 MW
V_{rms}	Rated rms line-line voltage	0.38 kV
R_s	Stator resistance	0.066 pu
R_r	Rotor resistance	0.103 pu
C_{bank}	Compensation capacitor	0.9 MVAR
P	Pole pairs	3
H	Mechanical time constant	2.5 sec

TABLE II
PARAMETERS OF THE RSFCL

Symbol	Quantity	Value
T_c	Critical temperature for HTS	90 °K
T_0	Temperature of cooling system	77 °K
I_{c0}	Critical current	5 kA
C_p	Specific heat of HTS	3 $MJm^{-3}K^{-1}$
P_{cool}	Power of cooling	300 kW
V_{SC}	HTS Volume	2e-3m^3
A_{SC}	HTS Cross section	3e-5m^2
ρ_n	Normal resistivity	4e-9 Ωm
ρ_f	Flux flow resistivity	1e-10 Ωm

Fig. 4 shows the current waveform of: 1) the load and the grid and 2) shunt active filter, in which the load current can be compensated by the shunt active filter current, keeping the grid current sinusoidal

To assess the operating characteristic and damping performance of the RSFCL, simulations based on the sample parameters ARE carried out for two scenarios: 1) without considering the SFCL, 2) with considering the SFCL. A symmetrical fault was considered at the integration point with the grid as illustrated in Fig. 1. The fault occurs at 1.1 s and cleared after 0.2 s.

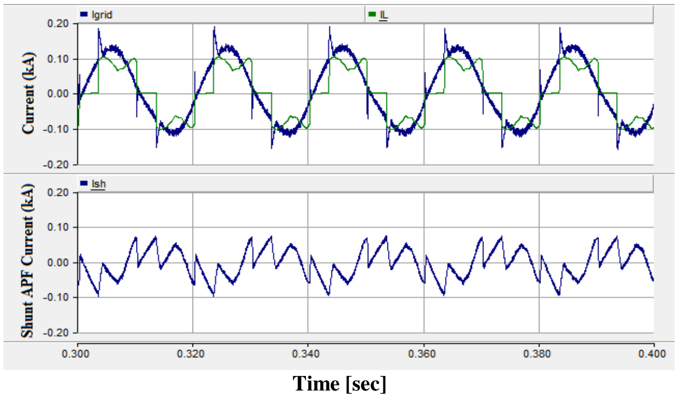

Fig 4. Current harmonics compensation. (a) Load and grid current. (b) Shunt active filter current.

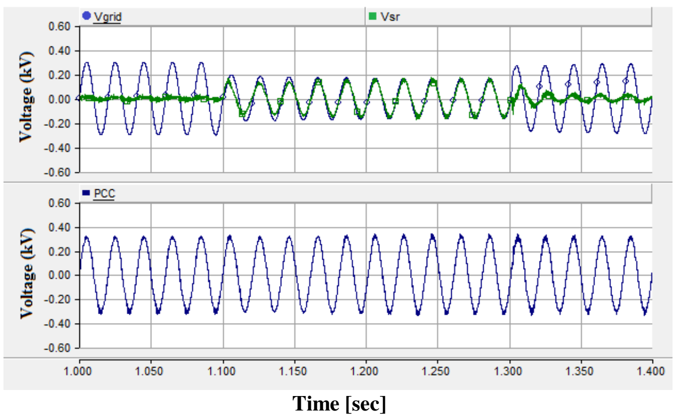

Fig 5. Voltage sags compensation without SFCL. (a) Grid voltage and series APF voltage. (b) PCC voltage with compensation.

For the results in this paper, the wind turbine operates at a wind speed of 13 m/s. In the absence of the SFCL, voltage sag of 50% occurs at grid bus. Fig. 5 (a) shows the grid voltage and voltage injected by series active filter and Fig. 5 (b) shows the PCC voltage which is kept in 1 pu.

The expediency of the SFCL component for managing the fault current as well as resistance and temperature variations of SFCL is demonstrated in Fig. 6. Before connecting SFCL, the peak of the current signal reaches about 14 kA for phase *a*. The installation of the SFCL on the main road by the wind farm will limit the maximum fault current effectively to reach about 10 kA in the first peak, and was further reduced to 6 kA in the third cycle.

A retrieval of the Fig 6(b) and (c) will determine, when a fault takes place at $t = 1.1$ s, the quench time (a transition from promising its superconducting mode to a resistive mode) is initiated by going through the flux-flow state during of 0.1 s and then to the normal state at a temperature rise of 90° K (critical temperature for HTS tap). Notwithstanding, this temperature rise requires around 0.4 s (20 cycles) for the HTS to reverse to its superconducting region, called restore time. Additionally, the limiting resistance of the SFCL went up to 0.003 Ω in the flux flow state and reached its normal state value of 0.023 Ω after ten cycles of the fault.

Fig. 7 shows the evolution of voltages at the wind turbine terminal with and without the SFCL. The impact of the installed SFCL on the voltage profile was significantly demon-

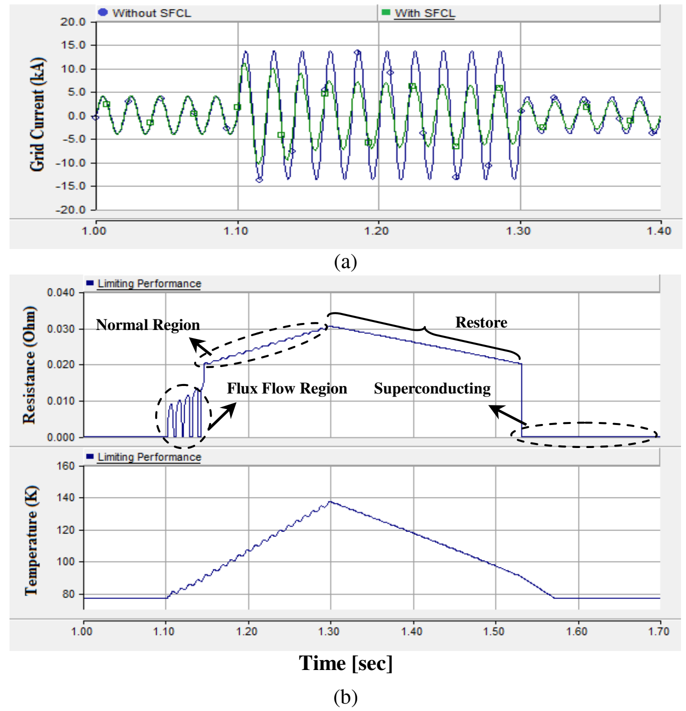

Fig 6. Performance evaluation of the SFCL model. (a) Fault current without and with SFCL in a single-phase system. (b) Resistance variation and temperature rise.

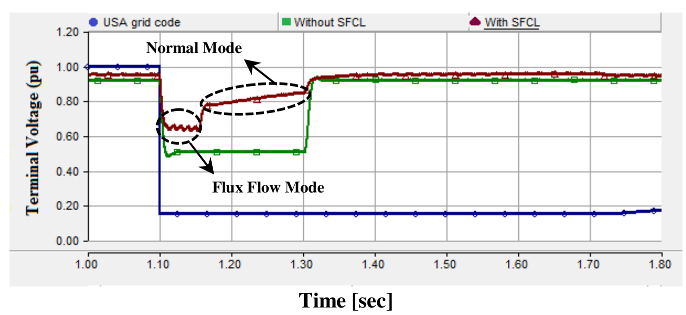

Fig 7. Voltage-dip characteristic at the generator terminal.

-strated by comparison of the voltage waveforms. The voltage sag was efficaciously improved by adding of the SFCL, reached 35% and 20% during the flux flow and normal state, respectively. It was observed that the PCC voltages recovered immediately to the nominal value upon clearing the fault.

Fig. 8 (a) shows the grid voltage and voltage injected by series active filter and Fig. 8 (b) shows the PCC voltage which is kept in 1 pu with SFCL. Fig. 9 shows a section of the simulated output active and reactive power with and without connecting SFCL. Before fault occurs, active power delivered to the grid is kept constant at the rated power 2MW with pitch angle control and the reactive power absorbed from the grid is kept at zero with capacitor bank. The active power drops to approximately 0.8 MW after fault occurred, without connecting SFCL. After connecting SFCL, the drop in the active power decreased, where it is attained about 1.25 MW.

VI. Conclusion

This paper has described the UPQC system to improve the power quality thereby to enhance low voltage ride-through capability of the FSIG-based wind turbine.

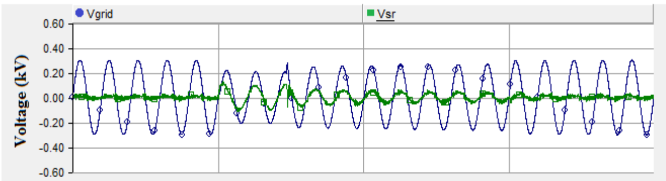

(a)

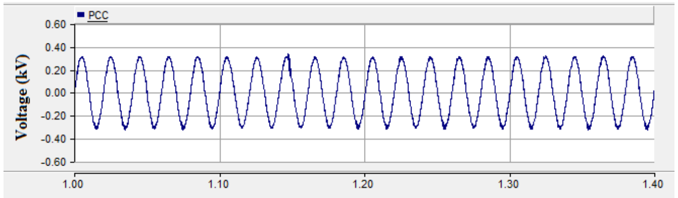

(b)

Time [sec]

Fig 8. Voltage sags compensation with SFCL. (a) Grid voltage and series APF voltage. (b) PCC voltage with compensation.

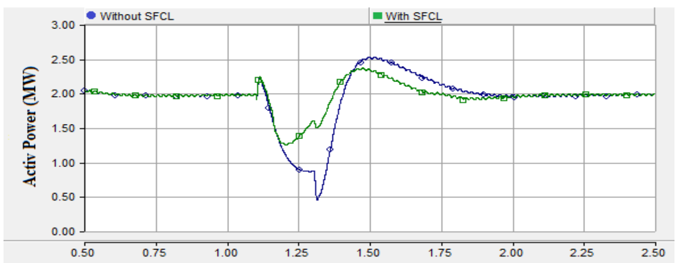

(a)

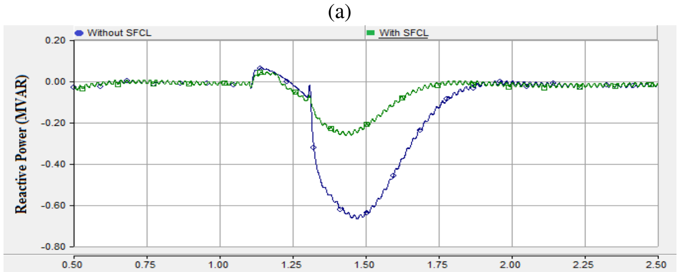

Time [sec]

(b)

Fig. 9. Active and reactive power delivered to the grid at PCC.

UPQC has the advantages of series and shunt APFs for compensating the distortions of grid voltages and load currents. Moreover, the application of superconducting fault current limiter in providing additional low voltage ride-through support to the wind-driven FSIG has been investigated. Utilizing RSFCL, the grid current has been limited effectively and the minimum voltage level at the generator terminal has been increased leading to compliance with international grid codes. Additionally, the overall dynamics of FSIG, represented by active and reactive power, have been improved by RSFCL. The results show that, the integration of FSIG-based wind turbine and UPQC system will become more promising from the energy-saving and downsizing perspective by introducing the RSFCL as self-healing limiter.

VII. References

[1] Federal Energy Regulatory Commission (FERC), United States of America, Docket no. RM05-4-000-Order no. 661, Interconnection for Wind Energy, Jun. 2, 2005.

[2] Mansour Mohseni, Syed M. Islam, "Review of international grid codes for wind power integration: Diversity, technology and a case for global standard," *Elsevier*, vol. 16, no. 6, pp. 3876–3890, August 2012.

[3] Muyeen, S. M. Ali, Mohd. Hasan, "Transient Stability Enhancement of Wind Generator by a New Logical Pitch Controller," *IEEE Trans. Power and Energy*, vol. 126, no. 8, pp. 742-752, 2006.

[4] Wessels, Hoffmann, Molinas, "StatCom control at wind farms with fixed-speed induction generators under asymmetrical grid faults,", *IEEE Trans. Industrial Electronics*, vol. 60, no. 7, pp. 2864, 2873, July 2013.

[5] N. Jayanti, M. Basu, M. Conlon, "Rating requirements of the UPQC to integrate the FSIG type wind generation to the grid," *IET renewable power generation,* vol. 3, no. 2, pp. 133-143, 2009.

[6] Hossain, M.J.; Pota, H.R.; Ugrinovskii, V.A.; Ramos, R.A., "Simultaneous STATCOM and Pitch Angle Control for Improved LVRT Capability of Fixed-Speed Wind Turbines,", *IEEE Trans. Sustainable Energy,* vol. 1, no. 3, pp. 142-151, Oct. 2010.

[7] Kinjo, T.; Senjyu, T.; Urasaki, N., "Terminal-voltage and output-power regulation of wind-turbine generator by series and parallel compensation using SMES," *Generation, Transmission and Distribution, IEE Proceedings*, vol. 153, no. 3, pp. 276-282, May 2006.

[8] H. Akagi, H. Fujita, "A new power line conditional for harmonic compensation in power systems," *IEEE Trans. Power Del*, vol. 10, no. 3, pp. 1570–1575, Jul. 1995.

[9] H. Fujita and H. Akagi, "Unified power quality conditioner: The integration of series and shunt active filter," IEEE Trans. Power Electron, vol. 13, no. 2, pp. 315–322, Mar. 1998.

[10] H.heydari, A.H, Moghadasi, "Optimization Scheme in Combinatorial UPQC and SFCL Using Normalized Simulated Annealing," *IEEE Trans, Power Delivery,* vol. 26, NO. 3, 2011.

[11] R. Sharifi, H. Heydari, "Multiobjective optimization for HTS fault current limiters based on normalized simulated annealing," *IEEE Trans. Appl. Superconduct*, vol. 19, no. 4, pp. 3675–3682, Aug. 2009.

[12] S. Heier, Grid Integration of Wind Energy Conversion Systems. Chicester: John Wiley & Sons, 1998.

[13] L. M. Fernandez et al, "Equivalent models of wind farms by using aggregated wind turbines and equivalent winds," Energy Conversion and Management, vol. 50, pp. 691–704, November 2008.

[14] E. S. Abdin and W. Xu, "Control design and dynamic performance analysis of a wind turbine-induction generator unit," *IEEE Trans. Energy Convers*, vol. 15, no. 1, pp. 91–96, Mar. 2000.

[15] B. Gromoll, G. Ries, W. Schmidt, H. Kramer, P. Kummeth, H. Neumuller, and S. Fischer, "Resistive current limiters with YBCO films," *IEEE Trans. Appl. Superconduct*, vol. 7, no. 2, pt. 1, pp. 828–831, Jun, 1997.

[16] D. K. Park, M. C. Ahn, S. E. Yang, Y. S. Yoon, B. Y. Seok, CLee, H. M. Chang, "Development of 220 V/300 A class non-inductive winding type fault current limiter using 2G HTS wire," *IEEE Trans. Appl. Superconduct*, vol. 17, no. 2, pt. 2, pp. 1863–1866, Jun, 2007.

[17] H. Shimizu and Y. Yokomizu, "A study on required volume of superconducting element for flux flow resistance type fault current limiter," *IEEE Trans. Appl. Superconduct*, vol. 13, no. 2, pp. 2052–2055, Jul, 2003.